Design, Manufacturing, and Testing Process of a Lab Scale Test Bench Hybrid Rocket Engine

Grigore Cican
Faculty of Aerospace Engineering, Polytechnic University of Bucharest, Romania | National Research and Development Institute for Gas Turbines COMOTI, Romania
grigore.cican@upb.ro (corresponding author)

Ionut Florian Popa
National Research and Development Institute for Gas Turbines COMOTI, Romania
ionut.popa@comoti.ro

Adrian Nicolae Buturache
FasterEdu, Romania
office@fasteredu.com

Andrei Iaroslav Hapenciuc
Vanguard Technology Association, Romania
andrei.hapenciuc@vanguard-technology.org

Received: 31 August 2023 | Revised: 21 September 2023 | Accepted: 26 September 2023

 DOI: https://doi.org/10.48084/etasr.6351

ABSTRACT

The current paper presents the architecture of a test bench for small (laboratory) scale hybrid rocket motors destined for teaching purposes. The sustainability of the proposed methodology is emphasized, as it addresses the development of small-scale hybrid rocket motor test benches, to be used either as didactic means for students or for research laboratories, by using low-cost materials, while preserving efficiency. In this regard, the entire development process is approached, from designing to manufacturing (including the casting of the fuel rod) and testing of the product. The developed product uses a mixture of 88% paraffin, 10% stearic acid, and 2% coal for the solid phase and liquid oxygen for the liquid phase. The testing of the hybrid rocket motor demonstrator was performed outdoors, in controlled conditions. The results showed a good correlation between the theoretical testing parameters with the obtained ones.

Keywords-test bench; hybrid rocket; manufacturing; propellant

I. INTRODUCTION

The early development of Hybrid Rocket Motors (HRMs) dates back to the 1930's [1], but only recently the research interest on this topic increased due to the cost-cutting demand related to the development of liquid engines and the safety concerns regarding solid propulsion systems. In the HRMs, once the oxidizer and fuel are placed in distinct parts of the propulsion system (usually, the oxidizer is in tanks and the solid fuel is stored in the combustion chamber), the possibility of explosion or detonation is further reduced [2]. HRMs offer many other advantages over liquid and solid systems, such as simplicity, reliability, start/stop/restart and Thrust-Vector Control (TVC) capabilities, low cost, higher specific impulse than solid rocket motors, and higher density-specific impulse than liquid bipropellant engines, while being environmentally friendly and flexible [3]. These benefits made it an attractive propulsion concept for scientific, and military, and commercial applications [4, 5].

One of the main issues preventing the widespread use of hybrid propulsion is the low regression rate of classical hybrid fuels. Paraffin-based fuel has been proposed as a viable solution, however, concerns regarding the thermomechanical properties of paraffin have often been seen as a possible obstacle. In [6], a small-scale hybrid rocket, capable of burning hydrogen peroxide and paraffin wax for an extended period, has been designed, built, and tested to investigate the suitability of paraffin wax as a hybrid fuel for actual missions. Most of the solid propellants used in the booster stages of the satellite launch vehicles produce large quantities of pollutants due to the fact that they are based on ammonium perchlorate, aluminum powder, and polybutadiene. Following combustion, these are producing large amounts of HCl and Al_2O_3 (e.g. Ariane 5 Booster [7], Titan II, Delta II, Space Shuttle [8]). There are

many studies related to the replacement of these solid propellants with other, less toxic ones. Authors in [9] presented a study of a solid propellant based on ADN/ETN/HTPB (ammonium dinitramide / erythritol tetranitrate / hydroxyl terminated polybutadiene), which gave, following its combustion, no HCl, or aluminum oxides, or ammonia result. Authors in [10] proposed a method to reduce the quantity of HCl resulting from solid propellants by using the effect of metal additives on neutralization and characteristics of AP/HTPB solid propellants. Another possible direction for green solid propellants would be the composite ones [11, 12]

An alternative to the solid rocket engines, and also the topic of the current paper, is the use of HRMs [13]. A retrospective of the worldwide status on using hybrid rocket motors for space transportation is presented in [14]. There have been several hybrid rocket propulsion systems operating, most known being SpaceShipOne in 2004 belonging to Scaled Composites [15] and HYSR in 2002 developed by Lockheed Martin [16]. Most HRMs are based on LO_x/HTPB, LO_x/paraffin, N_2O/paraffin, etc. [14]. As these have superior performances compared to the solid rocket engines and also they remove the issues associated to the generation of polluting substances, the use of LO_x and paraffin is of great interest for the development of efficient and environmentally friendly launch vehicles. Moreover, it is important that such preliminary studies can be performed at university and research institute level in order to increase the confidence in this technology and better assess its reliability. The current paper addresses this topic, by covering the entire process of developing a small-scale test bench for HRMs based on green propellants using paraffin.

Considering the attractive characteristics of HRMs described above, Université Libre de Bruxelles in collaboration with the Royal Military Academy of Belgium designed and manufactured a test bench to investigate a HRM that takes the advantage of the paraffin-based fuels and uses liquid N_2O as oxidizer [17]. In [18], the researchers documented the design details of a hybrid rocket test bench using plain hydroxyl terminated polybutadiene (HTPB) burning in gaseous oxygen (GOX). The test bench was designed to evaluate rocket motors with novel additives and formulations, along with their corresponding effects on regression rates and combustion efficiencies. Authors in [19] explored the throttling aspect of the HRM through experiments using a lab-scale motor. This one uses a wax-Al based fuel and compressed air as oxidizer. Author in [20] presented a design and laboratory experiment which was integrated in an introductive rocket propulsion university course. Thus, each student was tasked to develop a thrust hybrid rocket motor using HTPB and HTPB/Al solid fuel grains with gaseous oxygen as oxidizer. A similar approach is described in [21] which focused on the development of a test bench for rocket engines having educational purposes. The test bench was equipped for solid combustion as well as for hybrid engines with solid propellant and gaseous oxidizer. Authors in [22] presented a comprehensive review related to the research activities performed on the topic of HRM development at the Politecnico di Torino.

Compared to the literature on small-scale HRM test benches, the current work presents in a sustainable way the entire methodology to develop a test bench, covering design, component manufacturing, assembly, fuel bar manufacturing, instrumentation (including GUI), testing, and result analysis. This test bench is meant for teaching purposes, having low cost and high efficiency, thus being appropriate to be used in research laboratories, as well as in university dedicated courses.

II. MATERIALS AND METHODS

A. Design and Description of Parts and Components

The test bench design is modular, composed by many different small parts that can be changed when needed to meet the desired requirements. In Figure 1, a schematic of the whole test bench rocket is shown, in which the different blocks are clearly defined In this hybrid rocket model, 4 different parts can be clearly differentiated, namely two metal blocks (4) separated by the propellant block (2), the nozzle (1), and the metal fasteners (3). The test bench dimensions, the combustion chamber length, the diameter, and the nozzle dimensions [23] are presented in Figure 2.

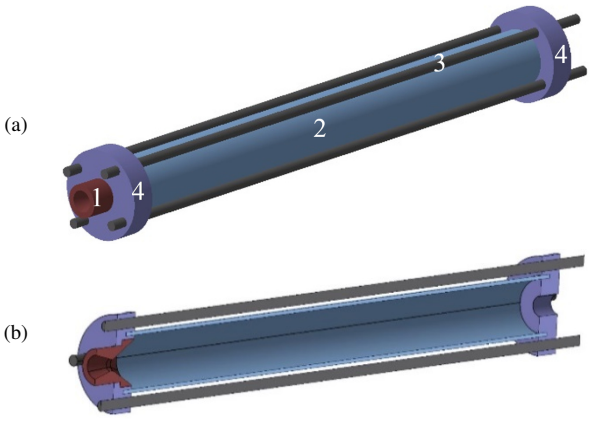

Fig. 1. HRM design: (a) isometric view, (b) section.

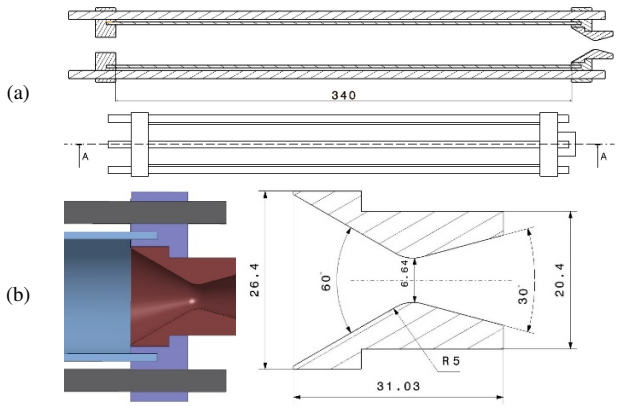

Fig. 2. Rocket motor overall dimensions: (a) section drawing, (b) nozzle.

The metal blocks separated by the propellant block can be seen in Figure 3.

Fig. 3. Rocket motor blocks.

B. Machining of the Parts

The components of the structural parts of the motor were manufactured from high temperature resistant steel AISI 310S for the nozzle (Figure 4) and AISI 304L for the sealing flanges and combustion chamber [24].

Fig. 4. Semifinished high temperature resistant steel (AISI 310S) bar before machining.

For the machining of the materials, the overall dimensions and the prescribed roughness are obtained by removing the machining allowance using appropriate tools. The machining of the parts was performed on a Mazak Nexus 150 lathe machine. The machining of the nozzle was performed as follows:

- The part was fixed in the lathe machine hydraulic spindle (Figure 5(a)).
- The part's radial runout was removed, followed by the drilling of a centering hole relative to the exterior surface (Figure 5(b)). This centering hole is used as reference for all the operations performed on this part.

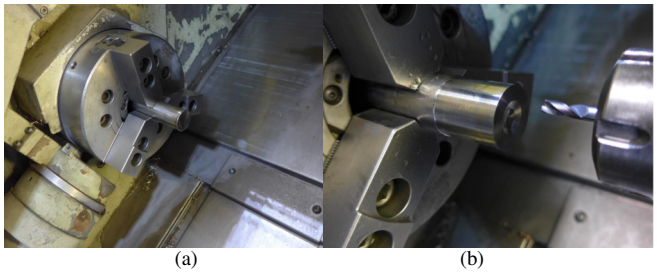

(a) (b)

Fig. 5. (a) Clamping the semifinished material in the lathe machine, (b) removing of the radial runout and drilling of the centering hole.

In order to obtain the nozzle inner profile, concentric holes were made using drill bits having nominal diameters between 6 and 12 mm (Figure 6(a)). This solution was adopted in order to reduce the manufacturing effort and time and to ensure a proper finishing of the nozzle inner profile. After performing the roughing of the part, three additional finishing operations were performed in order to remove the diameter shoulders (Figure 6). The following machining was performed on the outside part in order to obtain the final overall diameter of the nozzle outlet section and the final diameter of the nozzle in the area where it is welded on the corresponding sealing flange:

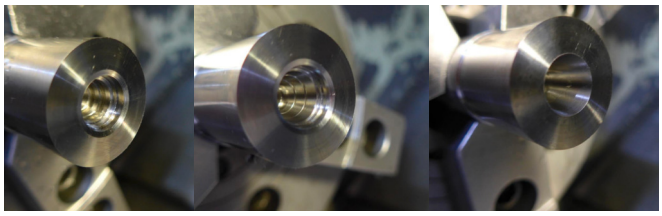

(a) (b) (c)

Fig. 6. (a) Nozzle inner surface after successive drilling with drill bits of 6, 8, 10, and 12 mm, (b) nozzle inner surface after the first finishing operation, (c) nozzle inner surface after all the finishing operations.

After finishing the machining for the nozzle side, the part was cut and clamped again on the lathe machine in order to perform the machining operations on the opposite side of the nozzle (Figure 7). This side was machined in the same way as the nozzle side, namely drilling successive holes followed by finishing operations in order to obtain the desired surface properties. The centering of the part is of high importance, as the surface obtained following the first part clamping shall be coinciding with the one resulting from the second clamping. After the part machining was completed, the desired nozzle inner profile was obtained.

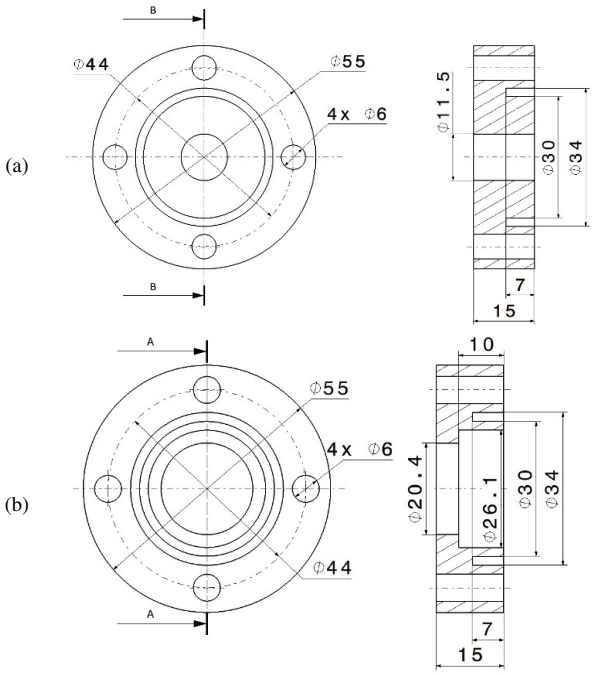

Fig. 7. (a) Nozzle sealing flange, (b) opposite side sealing flange (feeding area).

The semifinished part for the two flanges, AISI 304L, is fixed on the lathe machine hydraulic spindle, followed by drilling a centering hole (Figure 8). The centering hole was drilled on all the flange length, followed by performing the second inner diameter. After drilling the inner diameters of the nozzle flange, the part was cut to the desired length, and the manufacturing was continued with the second flange. After obtaining the desired diameter, the semifinished part was again

cut to obtain the second flange. In order to assemble the two flanges with the combustion chambers, machining of a concentric channel and 4 through holes for the threaded rods was required (Figure 9 left). Additionally, for the feeding flange, a G1/4 internal threaded port was made, in order to connect the oxygen supply to the combustion chamber (Figure 9 right). Following the nozzle and flange manufacturing, the nozzle was welded on the corresponding flange in order to allow the assembly with the combustion chamber (Figure 10).

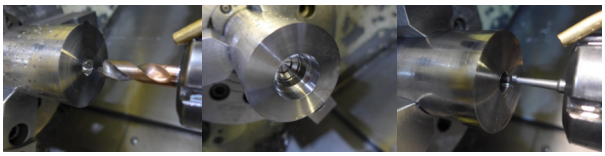

Fig. 8. Flange manufacturing steps.

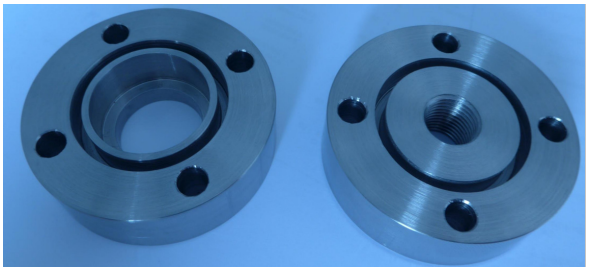

Fig. 9. The two flanges obtained following the machining.

Fig. 10. Welding of the nozzle on the corresponding flange.

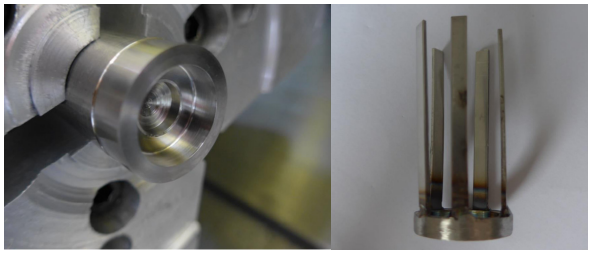

(a) (b)

Fig. 11. Fuel rod stopper: (a) machining on lathe, (b) final part after welding.

In order to ensure that inside the combustion chamber the fuel rod stays in the same position, a hard-stop feature was integrated in the design. This ring-shaped stopper is placed between the fuel rod and the nozzle, at 60 mm distance from the latter. The stopper is foreseen with 5 welded stripes made of high temperature resistant steel sheet (Figure 11). These stripes were later welded in certain points along the combustion chamber. For the two welding the WIG type welding was used. In order to measure the pressure and temperature at the nozzle inlet, two embossments were welded by WIG procedure at the fuel rod bottom. These embossments allow the integration of a pressure transducer and a thermocouple (Figure 12).

Fig. 12. Embossment welding for temperature and pressure measurement.

The two embossments have inner threads. In order to capture the desired parameters, holes were drilled both at the end which is in contact with the combustion chamber, as well as the combustion chamber itself. For the pressure transducer the hole was 4 mm, while for the thermocouple it was 2 mm.

C. Manufacturing of the Testing Fuel Rods and the Firing System

In order to validate the test bench, a mixture consisting of paraffin $C_{20}H_{42}$ (88%), stearic acid $C_{17}H_{36}O_2$ (10%), and coal powder $C_{71}H_3O_{13}N$ (2%) was used for the fuel rod. The paraffin cannot be used for HRMs without being enhanced [25]. Adding stearic acid and coal powder changes the behavior of the fuel rod [26] in the same way as for a composite material. Both the coal powder and the stearic acid improve the mechanical properties of the fuel rod, avoiding the detaching of large paraffin chunks which can block the nozzle and damage the rocket motor. Adding the coal powder also improves the integrity of the fuel rod, minimizes the radiative thermal transfer from the flame towards the fuel rod, and adds additional energy in the burning process. One can observe that the chemical compounds which are part of the reaction contain carbon, hydrogen, and oxygen, along with a small quantity of nitrogen. Thus, the products won't contain only combinations of them, making the fuel a green alternative, without any aluminum or chlorine compounds. The bars were casted in Plexiglas tubes, having the same inner diameter as the designed combustion chamber. The inner diameter of fuel rod was 10 mm (Figure 13).

The firing device consists of a mixture of potassium nitrate and sugar. This is one of the standard formulas used to ignite solid rocket engines made in rocketry challenges. According to Richard Nakka, a firing mixture made of 65% potassium nitrate and 35% sugar is the optimal solution for the used solid fuel. In order to increase the safety, the potassium nitrate amount is reduced, as the igniter performances are not of interest for the current paper (no rocket is launched). Thus, the chosen proportions were 60% potassium nitrate and 40% sugar. Additives could be used to enhance the igniting mixture in

order to increase the burning time or the generated heat quantity (corn syrup, aluminum powder, nitrocellulose). However, it was decided to follow the indications set forth by Richard Nakka in order to reduce the complexity related to the obtaining of the igniting mixture.

Fig. 13. Fuel rod ready for testing.

The ignition is made with nickeline wires powered by a 12 V source (Figure 14). When the current travels through the nickeline wire, the wire becomes incandescent, leading to the ignition of the mixture. It is mandatory that, when preparing an ignition mixture from potassium nitrate and sugar, the heating source temperature is maintained constant according to the manufacturing process. Most of the accidents linked to this process appear due to disregarding of this temperature indication or using an open flame instead of an electric stove.

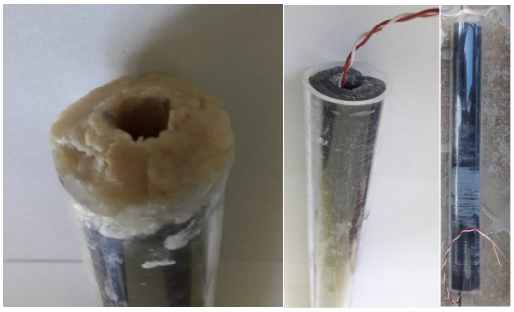

(a) (b)

Fig. 14. Rod ignition system: (a) potassium nitrate and sugar, (b) nickeline wires for ignition.

D. Test Bench Instrumentation

Below, the design of each block and part of the rocket highlighted in Figure 15 is explained in detail, as well as the reason behind its geometry and its main functions.

To achieve rigorous characterization of the rocket motor performance, a dedicated test bench and data acquisition and control system to comply with the accuracy and sampling speed requirements was designed and built. The possibility to use multiple type of sensors, depending on the rocket engine type was also taken into account. Figure 16 shows a block diagram of the data acquisition and control system.

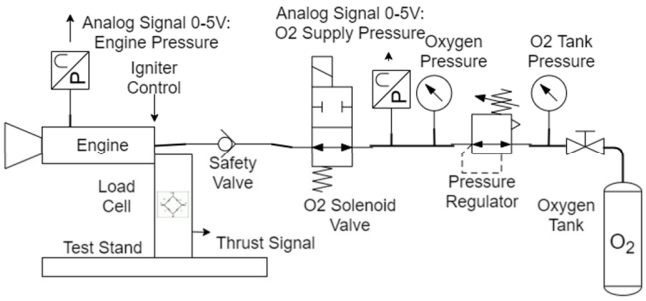

Fig. 15. Test bench block diagram.

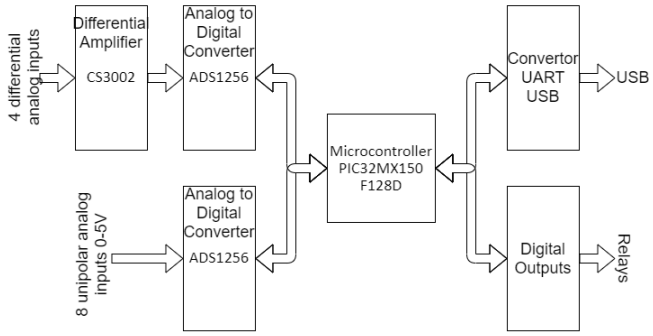

Fig. 16. Block diagram of the data acquisition and control system.

The test bench has a horizontal metallic frame and a vertical load cell. The motor is placed horizontally and pushes perpendicularly the load cell. In this way, the test bench size is reduced and the jet plume can be directed away from the pressurized oxygen tank. The maximum measuring force of the load cell is 250 kgf, and it was chosen to cover different rocket engine sizes, without compromising accuracy. The sensitivity of the load cell is 2 mV/V, meaning that, for an excitation voltage of 5 V, the maximum signal at 250 kg is 10mV. Estimating a 6-sigma accuracy of the data acquisition system of 0.4 uV, leads to a measurement accuracy of 10 g with a resolution of ~ 1 g, with a sampling period of 9.227 ms. Faster sampling speed is achievable, however with decreased accuracy. The data acquisition and control system has multiple interfaces to cover different setups:

- Four analog differential inputs to be used with sensors that use a resistive bridge, as load cells.
- Eight analog unipolar inputs with range of 0 – 5 V to be used with industrial sensors, as pressure sensors.
- Four digital inputs.
- Twelve high current open drain outputs to be used to drive external relays or DC motors.

The heart of the DAQ system is a 32 bit architecture, 50 Mhz microcontroller, part number PIC32MX150F128D (Figure 17).

For analog acquisition, the system relies on two ADS1256 delta sigma analog to digital converters that share the same SPI bus, but different chip select lines. The ADC accepts different power voltages for the digital and analog sides. Thus, a 5 V

analog power supply to have a 0-5V analog input range for 1 of the ADC used as 8 unipolar inputs was chosen. The second is used in a 4 differential input configuration.

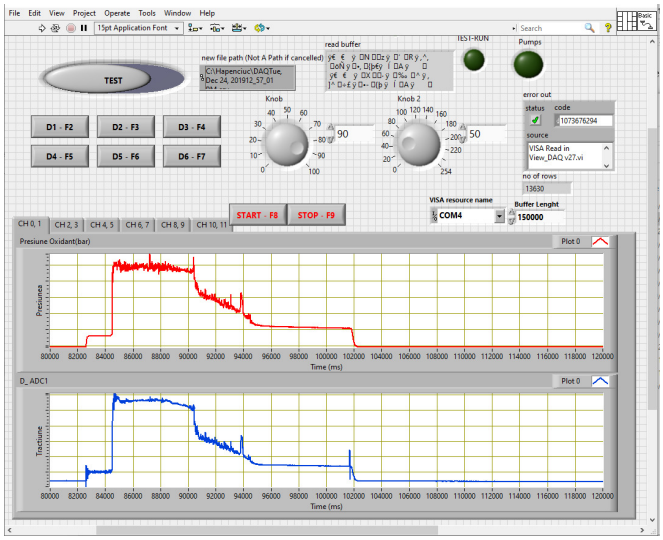

Fig. 17. DAQ GUI.

The differential inputs will be used from sensors that have a resistive bridge structure. They also provide an extremely low signal. For this reason, an extra differential amplifier was added to improve accuracy using CS3002 operational amplifier. The microcontroller sends the acquired data through USB to a miniPC where the parameters are recorded and displayed on a Graphical User Interface (GUI). The program can also send commands to the DAQ to control the O_2 flow or the igniter. The 12 analog inputs are displayed over 6 tabs, 2 plots per tab. The first tab presents pressure and thrust. The miniPC is connected to a WiFi network and it is accessed through a VNC connection. For the test, a 10 L and 200 bar O_2 tank was used. The pressure was reduced and kept constant during the test by using a Harris 825 pressure regulator set to keep a pressure of ~ 16 bar at the outlet. The pressure after the regulator is indicated on one of the gauges and also measured using a pressure transducer. The model used is able to measure 25 bars and it can be reused for tests requiring higher pressures. To turn on and off the O_2 flow, an ODE series 21H piloted solenoid valve is used. A second pressure transducer is mounted on the engine measurement port to record the pressure inside the combustion chamber (Figure 18).

Fig. 18. Pressure regulator, pressure transducer, and solenoid valve.

III. RESULTS AND DISCUSSION

The HRM assembly was made using threaded rods made of A2 stainless steel (equivalent to AISI 304). The flanges were secured on the rods using self-locking nuts (Figure 19). After component machining was finished, the assembly of the HRM followed, using all the components presented in Figure 19.

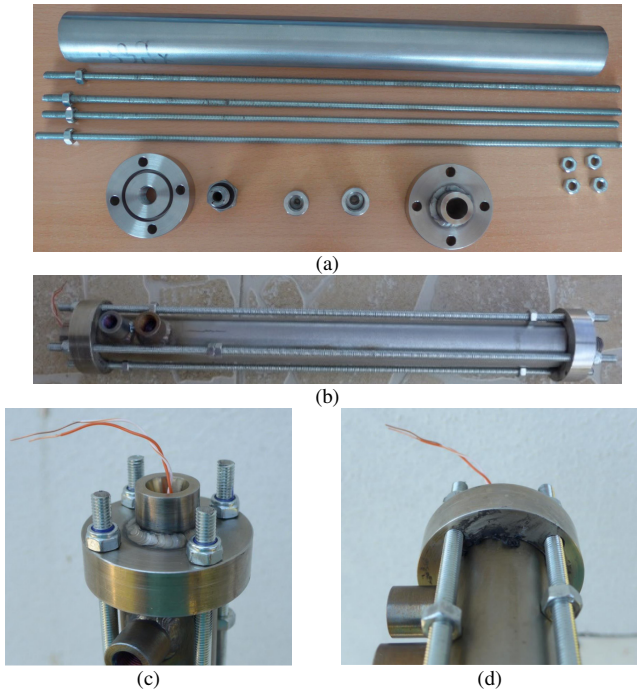

(a) (b) (c) (d)

Fig. 19. Assembly of the hybrid rocket motor in different stages: (a) components, (b) assembled rocket motor, (c) detail of the initiator rocket, (d) silicone-based sealing.

Fig. 20. Test bench with the integrated HRM after functioning.

For the sealing of the motor, it was decided to use a high temperature resistant sealant based on silicone (rated up to 1200 °C), which was introduced in the two flange channels (Figure 19(d)). It was assumed and accepted that, after the motor operation is stopped, the silicone sealing will be destroyed as a consequence of the thermal inertia. In order to validate the HRM and its test bench, the testing of the entire system was performed using the propellant mentioned above.

The configuration of the test bench with the rocket motor is presented in Figure 20. Following the tests performed, Figure 21 presents the variation of the thrust and the pressure inside the rocket engine.

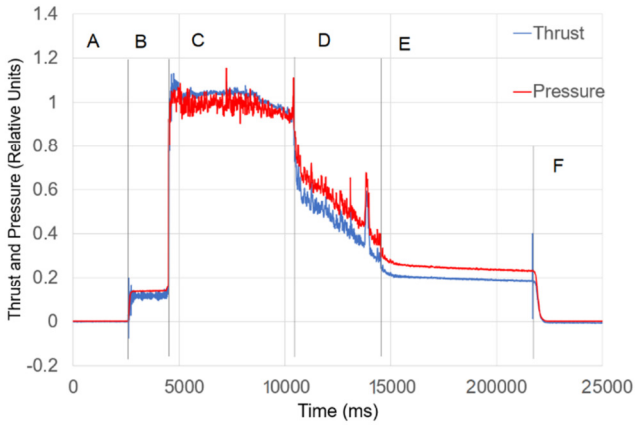

Fig. 21. Thrust and pressure plots over rocket engine functioning time.

The obtained test results show that the rocket engine worked without destroying itself, and the parameters obtained correspond to those resulting from the theoretical models from the literature. From Figure 21, there are 6 visible time periods with different pressure thrust levels:

- A: Oxygen flow is off and the igniter is off.
- B: Oxygen flow is on, the igniter is off, the motor acts as a cold jet thruster with low pressure and low thrust.
- C: Igniter is fired and combustion starts. Pressure and thrust increase significantly and are kept almost constant. The burn is very clean, the flame is invisible in the video, probably because of high O/F ratio.
- D: Pressure and thrust are decreasing gradually. In video capture, the flame becomes visible, accompanied by shock diamonds. Some spikes are identified in the recording, probably indicating that some fuel may have detached from the internal surface of the combustion chamber.
- E: the fuel is fully consumed. Thrust and pressure are caused only by oxygen flow. Levels are significantly higher than in B interval because the hot combustion chamber is increasing the temperature of the oxygen.
- F: Solenoid valve cuts the oxygen flow. The test is complete.

IV. CONCLUSIONS

In this paper, design, manufacturing, and testing of a hybrid rocket motor using green propellant based on paraffin was presented step by step as an accessible, easy to achieve, and low-cost process. Compared to other literature works, the current study presents the manufacturing process, step by step, for the entire laboratory model of the rocket motor, including the fabrication of the fuel rods and the ignition system. The obtained experimental results are in accordance to those obtained from calculations. The laboratory test bench is accessible and it can be used to train and help future researchers and students of the Polyethnic University of Bucharest, Faculty of Aerospace Engineering, in their quest to assess and find new alternatives for rocket fuels which are also environmentally friendly.

At the moment the article was written and to the best of our knowledge, there was no other scientific article comprehensive enough that provides end to end guidance on hybrid rocket engine design, manufacturing, and testing. All these three major phases needed to achieve the main goal of the article are having the right level of detail in order to ensure other researchers can repeat the experiments with similar results.

For future work, it is proposed to assess the mechanical properties of the paraffin (tensile force, compression, and torsion, all visualized using a scanning electron microscope) at room temperature and at negative temperatures compared to the recipe proposed in this study.

ACKNOWLEDGMENT

The paper was realized with the help of the NUCLEU program, as part of the National Strategy for Research, Development and Innovation, carried out with the support of the Ministry of Research, Innovation and Digitalization, project no. PN 23.12.06.02.

REFERENCES

[1] M. Calabro, "Overview on hybrid propulsion," in *Progress in Propulsion Physics*, Versailles, France, 2011, vol. 2, pp. 353–374, https://doi.org/10.1051/eucass/201102353.

[2] K. K. Kuo and M. J. Chiaverini, *Fundamentals of Hybrid Rocket Combustion and Propulsion*. 2007: American Institute of Aeronautics and Astronautics, 2007, https://doi.org/10.2514/4.866876.

[3] G. P. Sutton and O. Biblarz, *Rocket Propulsion Elements*, 9th ed. Hoboken, NJ, USA: Wiley, 2016.

[4] D. Bianchi, F. Nasuti, and C. Carmicino, "Hybrid Rockets with Axial Injector: Port Diameter Effect on Fuel Regression Rate," *Journal of Propulsion and Power*, vol. 32, no. 4, pp. 984–996, Jul. 2016, https://doi.org/10.2514/1.B36000.

[5] E. Toson and A. M. Karabeyoglu, "Design and Optimization of Hybrid Propulsion Systems for In-Space Application," in *51st AIAA/SAE/ASEE Joint Propulsion Conference*, Orlando, FL, USA, Jul. 2015, https://doi.org/10.2514/6.2015-3937.

[6] M. Santi *et al.*, "Development and Testing of a Long Burning Time Lab-scale Paraffin-based Hybrid Rocket Motor," in *53rd AIAA/SAE/ASEE Joint Propulsion Conference*, Atlanta, GA, USA, Jul. 2017, https://doi.org/10.2514/6.2017-4829.

[7] "Boosters (EAP)," *The European Space Agency*. https://www.esa.int/Enabling_Support/Space_Transportation/Launch_vehicles/Boosters_EAP.

[8] J. A. Dallas, S. Raval, J. P. Alvarez Gaitan, S. Saydam, and A. G. Dempster, "The environmental impact of emissions from space launches: A comprehensive review," *Journal of Cleaner Production*, vol. 255, May 2020, Art. no. 120209, https://doi.org/10.1016/j.jclepro.2020.120209.

[9] G. Cican and A. D. Mitrache, "Rocket Solid Propellant Alternative Based on Ammonium Dinitramide," *INCAS Bulletin*, vol. 9, no. 1, pp. 17–24, Mar. 2017, https://doi.org/10.13111/2066-8201.2017.9.1.2.

[10] U. Vellaisamy and S. Biswas, "Effect of metal additives on neutralization and characteristics of AP/HTPB solid propellants," *Combustion and Flame*, vol. 221, pp. 326–337, Nov. 2020, https://doi.org/10.1016/j.combustflame.2020.08.006.

[11] H. Naseem, J. Yerra, H. Murthy, and P. A. Ramakrishna, "Ageing studies on AP/HTPB based composites solid propellants," *Energetic Materials Frontiers*, vol. 2, no. 2, pp. 111–124, Jun. 2021, https://doi.org/10.1016/j.enmf.2021.02.001.

[12] A. Mukhtar and H. Nasir, "Comparative Closed Vessel Firing-Ballistic Parameters Evaluation for Development of Base Bleed Composite Solid Propellant," *Engineering, Technology & Applied Science Research*, vol. 8, no. 6, pp. 3545–3549, Dec. 2018, https://doi.org/10.48084/etasr.2370.

[13] Ş. Predoi, Ş. Grigorean, and G. Dumitraşcu, "The Regression Rate-Based Preliminary Engineering Design of Hybrid Rocket Combustion System," *Processes*, vol. 10, no. 4, Apr. 2022, Art. no. 775, https://doi.org/10.3390/pr10040775.

[14] A. Okninski, W. Kopacz, D. Kaniewski, and K. Sobczak, "Hybrid rocket propulsion technology for space transportation revisited - propellant solutions and challenges," *FirePhysChem*, vol. 1, no. 4, pp. 260–271, Dec. 2021, https://doi.org/10.1016/j.fpc.2021.11.015.

[15] E. Seedhouse, "SpaceShipOne," in *Virgin Galactic: The First Ten Years*, E. Seedhouse, Ed. Cham, Germany: Springer International Publishing, 2015, pp. 33–63.

[16] J. Arves, M. Gnau, D. Kearney, and K. Joiner, "Hybrid Sounding Rocket(HYSR)Program," in *39th AIAA/ASME/SAE/ASEE Joint Propulsion Conference and Exhibit*, Huntsville, AL, USA, Jul. 2003, https://doi.org/10.2514/6.2003-5199.

[17] M. Bouziane, A. E. De Morais Bertoldi, P. Milova, P. Hendrick, and M. Lefebvre, "Development and Testing of a Lab-scale Test-bench for Hybrid Rocket Engines," in *2018 SpaceOps Conference*, Marseille, France, May 2018, https://doi.org/10.2514/6.2018-2722.

[18] J. C. Thomas, J. M. Stahl, G. R. Morrow, and E. L. Petersen, "Design of a Lab-Scale Hybrid Rocket Test Stand," in *52nd AIAA/SAE/ASEE Joint Propulsion Conference*, Jul. 2016, https://doi.org/10.2514/6.2016-4965.

[19] A. Bhadran, J. G. Manathara, and P. A. Ramakrishna, "Thrust Control of Lab-Scale Hybrid Rocket Motor with Wax-Aluminum Fuel and Air as Oxidizer," *Aerospace*, vol. 9, no. 9, Sep. 2022, Art.l no. 474, https://doi.org/10.3390/aerospace9090474.

[20] A. J. Marchese, "Work In Progress: This is Rocket Science: Development and Testing of a Hybrid Rocket Motor in a Rocket Propulsion Course," in *Proceedings. Frontiers in Education. 36th Annual Conference*, San Diego, CA, USA, Jul. 2006, pp. 17–18, https://doi.org/10.1109/FIE.2006.322639.

[21] T. Neff, M. Rehberger, and A. Meroth, "Thrust test bench for student rocket engines," in *2016 11th France-Japan & 9th Europe-Asia Congress on Mechatronics (MECATRONICS) /17th International Conference on Research and Education in Mechatronics (REM)*, Jun. 2016, pp. 141–145, https://doi.org/10.1109/MECATRONICS.2016.7547130.

[22] L. Casalino, F. Masseni, and D. Pastrone, "Hybrid Rocket Engine Design Optimization at Politecnico di Torino: A Review," *Aerospace*, vol. 8, no. 8, Aug. 2021, Art. no. 226, https://doi.org/10.3390/aerospace8080226.

[23] M. W. Khalid and M. Ahsan, "Computational Fluid Dynamics Analysis of Compressible Flow Through a Converging-Diverging Nozzle using the k-ε Turbulence Model," *Engineering, Technology & Applied Science Research*, vol. 10, no. 1, pp. 5180–5185, Feb. 2020, https://doi.org/10.48084/etasr.3140.

[24] S. Anjum, M. Shah, N. A. Anjum, S. Mehmood, and W. Anwar, "Machining and Surface Characteristics of AISI 304L After Electric Discharge Machining for Copper and Graphite Electrodes in Different Dielectric Liquids," *Engineering, Technology & Applied Science Research*, vol. 7, no. 4, pp. 1765–1770, Aug. 2017, https://doi.org/10.48084/etasr.1250.

[25] Y. Pal, S. K. Palateerdham, S. N. Mahottamananda, S. Sivakumar, and A. Ingenito, "Combustion performance of hybrid rocket fuels loaded with MgB2 and carbon black additives," *Propulsion and Power Research*, vol. 12, no. 2, pp. 212–226, Jun. 2023, https://doi.org/10.1016/j.jppr.2022.11.003.

[26] E. Toson, M. Kobald, E. Cavanna, L. T. D. Luca, G. Consolati, and H. Ciezki, "Feasibility Study of Paraffin-Based Fuels for Hybrid Rocket Engine Applications," *International Journal of Energetic Materials and Chemical Propulsion*, vol. 13, no. 6, pp. 559–572, 2014, https://doi.org/10.1615/IntJEnergeticMaterialsChemProp.2014011243.